



2

AEROSPACE REPORT NO.  
TR-0091(6940-09)-2

## A Molecule-Specific Filter Modulator

Prepared by

J. T. KNUDTSON, T. M. REESE, AND K. C. HERR  
Space and Environment Technology Center

15 September 1991

Prepared for

SPACE SYSTEMS DIVISION  
AIR FORCE SYSTEMS COMMAND  
Los Angeles Air Force Base  
P. O. Box 92960  
Los Angeles, CA 90009-2960

DTIC  
ELECTE  
MAY 28 1992  
S D

Engineering and Technology Group

92-13946



THE AEROSPACE CORPORATION  
El Segundo, California

92 5 27 030

APPROVED FOR PUBLIC RELEASE  
DISTRIBUTION UNLIMITED

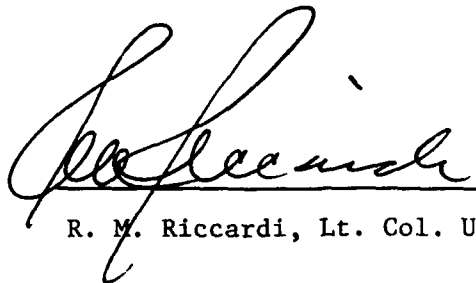
This report was submitted by The Aerospace Corporation, El Segundo, CA 90245-4691, under Contract No. F04701-88-C-0089 with the Space Systems Division, P. O. Box 92960, Los Angeles, CA 90009-2960. It was reviewed and approved for The Aerospace Corporation by A. B. Christensen, Principal Director, Space and Environment Technology Center. Lt. Col. Riccardi was the project officer for the Mission-Oriented Investigation and Experimentation (MOIE) program

This report has been reviewed by the Public Affairs Office (PAS) and is releasable to the National Technical Information Service (NTIS). At NTIS, it will be available to the general public, including foreign nationals.

This technical report has been reviewed and is approved for publication. Publication of this report does not constitute Air Force approval of the report's findings or conclusions. It is published only for the exchange and stimulation of ideas.



Martin K. Williams, Capt. USAF  
MOIE Project Manager



R. M. Riccardi, Lt. Col. USAF, BSC

UNCLASSIFIED

SECURITY CLASSIFICATION OF THIS PAGE

## REPORT DOCUMENTATION PAGE

1a. REPORT SECURITY CLASSIFICATION Unclassified			1b. RESTRICTIVE MARKINGS			
2a. SECURITY CLASSIFICATION AUTHORITY			3. DISTRIBUTION/AVAILABILITY OF REPORT  Approved for public release; distribution unlimited			
2b. DECLASSIFICATION/DOWNGRADING SCHEDULE						
4. PERFORMING ORGANIZATION REPORT NUMBER(S) TR-0091(6940-09)-2			5. MONITORING ORGANIZATION REPORT NUMBER(S) SSD-TR-92-05			
6a. NAME OF PERFORMING ORGANIZATION The Aerospace Corporation Technology Operations	6b. OFFICE SYMBOL (If applicable)		7a. NAME OF MONITORING ORGANIZATION Space Systems Division			
6c. ADDRESS (City, State, and ZIP Code) El Segundo, CA 90245-4691			7b. ADDRESS (City, State, and ZIP Code) Los Angeles Air Force Base Los Angeles, CA 90009-2960			
8a. NAME OF FUNDING/SPONSORING ORGANIZATION	8b. OFFICE SYMBOL (If applicable)		9. PROCUREMENT INSTRUMENT IDENTIFICATION NUMBER F04701-88-C-0089			
8c. ADDRESS (City, State, and ZIP Code)			10. SOURCE OF FUNDING NUMBERS			
			PROGRAM ELEMENT NO.	PROJECT NO.	TASK NO.	WORK UNIT ACCESSION NO.
11. TITLE (Include Security Classification) A Molecule-Specific Filter Modulator						
12. PERSONAL AUTHOR(S) Knudtson, J. T., Reese, T. M., and Herr, K. C.						
13a. TYPE OF REPORT		13b. TIME COVERED FROM _____ TO _____		14. DATE OF REPORT (Year, Month, Day) 1991 September 15		
15. PAGE COUNT 28						
16. SUPPLEMENTARY NOTATION						
17. COSATI CODES			18. SUBJECT TERMS (Continue on reverse if necessary and identify by block number)			
FIELD	GROUP	SUB-GROUP	Fabry-Perot Filter Weak IR Detection Spectral Dithering			
19. ABSTRACT (Continue on reverse if necessary and identify by block number)						
<p>An optical Fabry-Perot filter has been devised to aid in the detection of weak infrared emission from hot molecules. The comb-like transmission spectrum of the filter was matched to the comb-like infrared emission spectrum of CO. (Other small molecules are also suitable.) The filter can be made to perform rapid background subtraction by slightly detuning the filter spectrum from the molecular emission spectrum. This invention is called spectral dithering and can be performed at rates up to several kilohertz using a piezoelectrically driven Fabry-Perot. In cases where atmospheric fluctuations are a significant noise source, background subtraction at kilohertz rates can essentially "freeze" the fluctuations. This improves the effectiveness of the background subtraction. Estimates of the signal/background and signal/noise improvements for the filter are given. The spectral dithering capability was demonstrated in a laboratory experiment using CO emission from a flame.</p>						
20. DISTRIBUTION/AVAILABILITY OF ABSTRACT			21. ABSTRACT SECURITY CLASSIFICATION			
<input checked="" type="checkbox"/> UNCLASSIFIED/UNLIMITED <input type="checkbox"/> SAME AS RPT. <input type="checkbox"/> DTIC USERS			Unclassified			
22a. NAME OF RESPONSIBLE INDIVIDUAL			22b. TELEPHONE (Include Area Code)		22c. OFFICE SYMBOL	

## PREFACE

We thank J. B. Koffend and B. P. Kasper for calculating the convolution integrals and making the plots for Figs. 5, A1 and A2.



Accession For	
NTIS GRA&I	<input checked="checked" type="checkbox"/>
DTIC TAB	<input type="checkbox"/>
Unannounced	<input type="checkbox"/>
Justification	
By _____	
Distribution/	
Availability Codes	
Dist	Avail and/or Special
A-1	

## CONTENTS

I. INTRODUCTION .....	5
II. A HEURISTIC EXAMPLE .....	9
III. DETECTING CO IN A ROCKET PLUME .....	11
IV. SPECTRAL DITHERING .....	15
V. DEVELOPMENT OF AN FP FILTER FOR CO (CARBON MONOXIDE) .....	19
VI. SPECTRAL DITHERING DEMONSTRATION .....	21
VII. SUMMARY .....	23
REFERENCES .....	25
APPENDIX .....	27

## FIGURES

1.	Fabry-Perot Interferometer .....	5
2.	Spectrally Dithered Comb Filter .....	6
3.	Background Emission Spectrum .....	11
4.	Signal Emission Spectrum .....	12
5.	(a) Fabry-Perot Modulated Signal Spectrum, finesse = 25 (b) Fabry-Perot Modulated Background Spectrum, finesse = 25..	13
6.	Atmospheric Modulation Spectrum .....	16
7.	Measurement of FP Finesse of 31.3 with CO Laser at 5.32 $\mu\text{m}$ .....	19
8.	FP Modulated Emission Spectrum for a Small Gas Flame .....	21
A1a.	Fabry-Perot Modulated Signal Spectrum (finesse = 50) .....	27
A1b.	Fabry-Perot Modulated Background Spectrum (finesse = 100)..	27
A2a.	Fabry-Perot Modulated Signal Spectrum (finesse = 100) .....	28
A2b.	Fabry-Perot Modulated Background Spectrum (finesse = 100) .....	28

## TABLE

1.	Signal and Background With and Without Fabry-Perot Filter .....	14
----	---	----

## I. INTRODUCTION

The vibration-rotation emission spectra of small molecules consist of a series of almost-regularly spaced lines. The emission lines are generally spaced far apart ( $1$  to  $20\text{ cm}^{-1}$ ) compared with their width ( $0.1$  to  $0.01\text{ cm}^{-1}$ ). Typically, most of the power is emitted in a few tens of these vibration-rotation lines. Infrared emissions from hot molecules are usually detected with a bandpass transmission filter that overlaps the strongest lines. However, when the signal (the molecular emission) is weak, the transmitted background radiation can become a major noise source. This is because the background radiation occurs at all wavelengths, while the molecular emission is restricted to discrete line wavelengths. The result can be a weak picket fence emission spectrum superimposed on a fluctuating background continuum. A significant improvement in detectability can be gained if one can devise a method of looking only where the molecular emissions are located. In order to accomplish this, we propose using a Fabry-Perot (FP) interference filter.

The transmission spectrum of an interferometer consists of a series of regularly spaced transmission peaks. Figure 1 shows a schematic diagram of a Fabry-Perot (upper portion) and its transmission spectrum (lower portion). The locations of the peaks are determined by the distance ( $\ell$ ) between the two partially reflecting mirrors. The width of the peaks is determined by the reflectance of the two mirrors. The comb-like transmission spectrum of the filter will reduce the background while still transmitting the molecular emission.

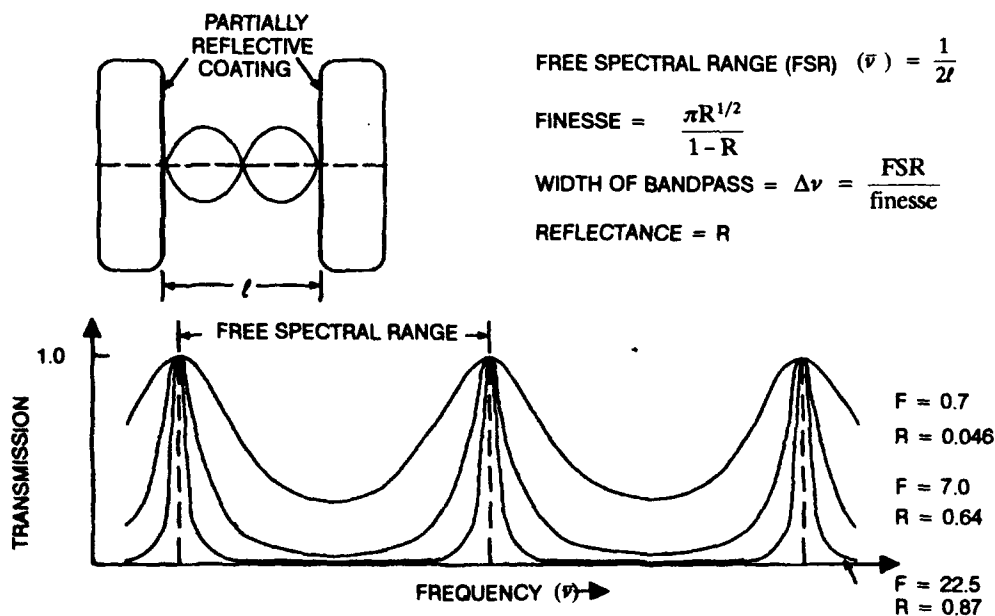


Figure 1. Fabry-Perot Interferometer

Matching the FP transmission spectrum to the CO<sub>2</sub> emission spectrum was proposed for satellite measurement of the temperature in the upper atmosphere in 1961.<sup>1,2</sup> More recently, Randall et al. have calculated and measured the ability of an FP filter to detect the infrared emission lines from water vapor emission in the presence of a blackbody background.<sup>3,4</sup> The H<sub>2</sub>O emission spectrum is relatively complex and significantly anharmonic (not regularly spaced) so that the overlap of the FP filter and the H<sub>2</sub>O lines was far from ideal. Randall et al. concluded that the system would work much better for more harmonic emitters like carbon monoxide.

We have invented a significant improvement to the FP filter, which we call spectral dithering. The positions of all of the peaks in the FP spectrum can be shifted simultaneously. This is done by very slightly displacing one of the two FP mirrors with a piezoelectric drive. This is shown schematically in Fig. 2. In position 1, the FP transmission peaks overlap the four molecular emission lines. In position 2, they overlap just the background continuum emission. The shift between the two positions can be made very rapidly—in less than one millisecond.

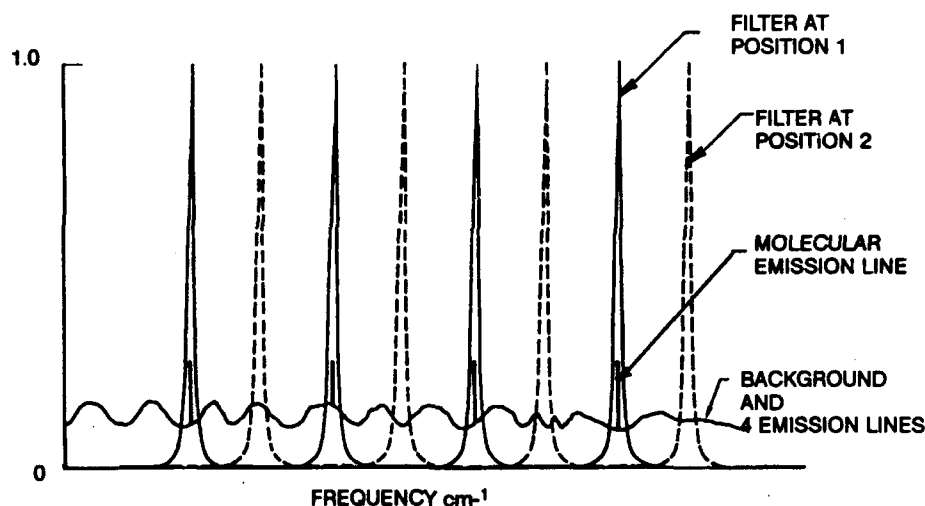


Figure 2. Spectrally Dithered Comb Filter.

Spectral dithering improves the signal/noise ratio in two ways. First, it is a background subtraction technique. The spectral dithering produces an AC signal at the detector whose amplitude is proportional to the molecular emission.

$$\text{dithered signal amplitude} = (\text{background} + \text{molecular emission}) - (\text{background})$$

Second, the time between the two measurements is short (~ 1 millisecond), essentially freezing the radiometric fluctuations in the background emission. These fluctuations typically have a 1/f frequency dependence that reaches a minimum at frequencies greater than a few hundred hertz.



The spectrally dithered FP also has an important molecular recognition advantage. It discriminates between the target molecule emission spectrum and other sources of radiation in the wavelength region of interest. Consider the signal from a hot blackbody in the field of view. The blackbody emission spectrum is an almost flat continuum over a 50 to 100  $\text{cm}^{-1}$  region in which the target molecule emits. Therefore, the power transmitted by the FP picket fence spectrum is the same in both the overlap and non-overlap positions. Since the signal level is identical in both positions, there is no AC signal.

The AC signal from the FP filter is a "fingerprint" of the source emission spectrum. In essence, the FP verifies that the emission source is the target molecule and greatly reduces the probability of false target detections.

## II. A HEURISTIC EXAMPLE

As an example, consider a telescope attempting to detect an infrared emitting propulsion system above the atmosphere. The optical system typically includes a bandpass filter centered around a molecular emission band. The hot exhaust gases produce a signal level of 1 in the presence of a sky background level of 100. Typically, the telescope points to a region of the sky with just background (level = 100) and then to the region containing the signal and background (level = 101). If the background level is constant in both views, the signal can be obtained by subtraction. This is called spatial dithering. However, if there is a 1% fluctuation in the background during the two views, the noise is now 1% of 100 and the signal-to-noise ratio is 1:1. Therefore, the noise in this system depends on both the amount of background power transmitted by the filter and on the percent of fluctuation in the background during the dithering process. Typically on large telescopes, the secondary mirror is dithered at a frequency of 10 Hz. In general, this dither rate is not sufficient to completely eliminate the atmospheric turbulence effects. Higher frequencies are more desirable since the knee of the atmospheric seeing curve is at approximately 200 Hz.

We have considered the effect of applying the proposed FP filter to this example. Model calculations (described below) show that the signal-to-background ratio is increased as much as 13.5 by the FP filter. However, the signal-to-noise ratio will be increased even further because the fluctuations in the background will be less than 1% during the FP spectral modulation time of a millisecond. If the fluctuation were reduced by a factor of 10, then the total signal-to-noise ratio would be increased by 135.

### III. DETECTING CO IN A ROCKET PLUME

We have calculated the performance of an FP system viewing a liquid  $\text{H}_2/\text{O}_2$  fueled propulsion system operating above the atmosphere. Carbon monoxide (CO) constitutes about 7 mole percent of the exhaust gases. The  $\Delta v = -1$  vibrational transitions are responsible for most of the infrared emission from CO. The  $v = 1 \rightarrow 0$  transition is the most intense, but it is strongly attenuated by atmospheric CO absorptions and, therefore, appears very weak below the earth's atmosphere. However, the emission from the next higher level,  $v = 2 \rightarrow 1$ , is transmitted by the atmosphere because the  $2 \rightarrow 1$  transitions do not overlap the  $v = 1 \rightarrow 0$  transitions. In this example, the FP will be used to detect the hot CO  $v = 2 \rightarrow 1$  emissions, while rejecting background emission (including the atmospheric CO  $v = 1 \rightarrow 0$  emissions).

Figure 3 shows the background emission spectrum from atmospheric CO in the 2135 to 2175  $\text{cm}^{-1}$  region. It was calculated using the Hitran program. The total power emitted by the background is 77 (arbitrary units).

The target emission spectrum is shown in Fig. 4. It was calculated using a computer combustion model for the liquid  $\text{H}_2/\text{O}_2$  propulsion system. The absorption of the atmosphere has been included in Fig. 4. Some of the emission peaks in the target spectrum are about as strong as the peaks in the background spectrum. However, the total power emitted by the target spectrum is only 1.0 (arbitrary units) compared with the 77 emitted by the background. Therefore, the signal-to-background ratio is  $1.0/77 = 0.013$ .

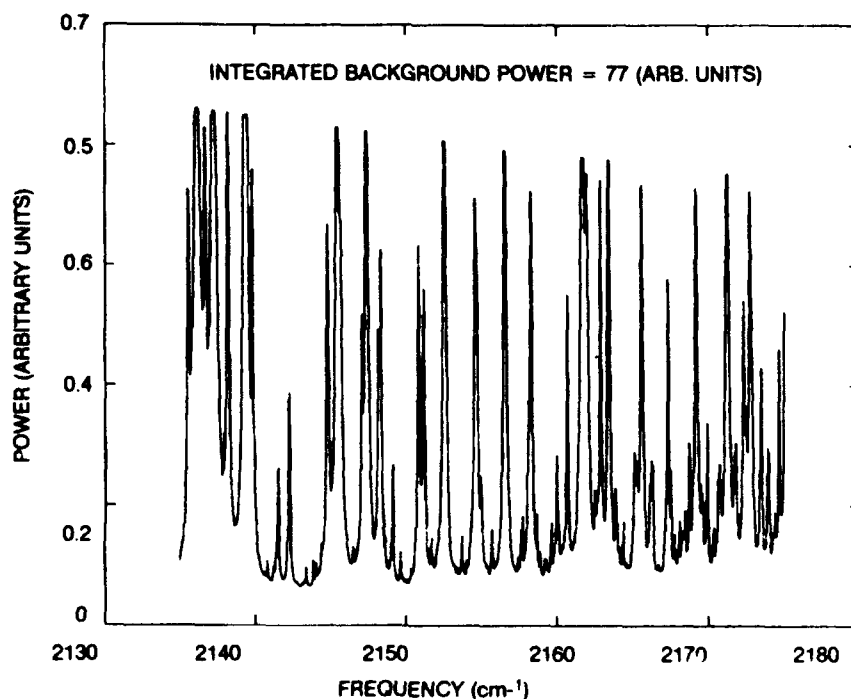


Figure 3. Background Emission Spectrum

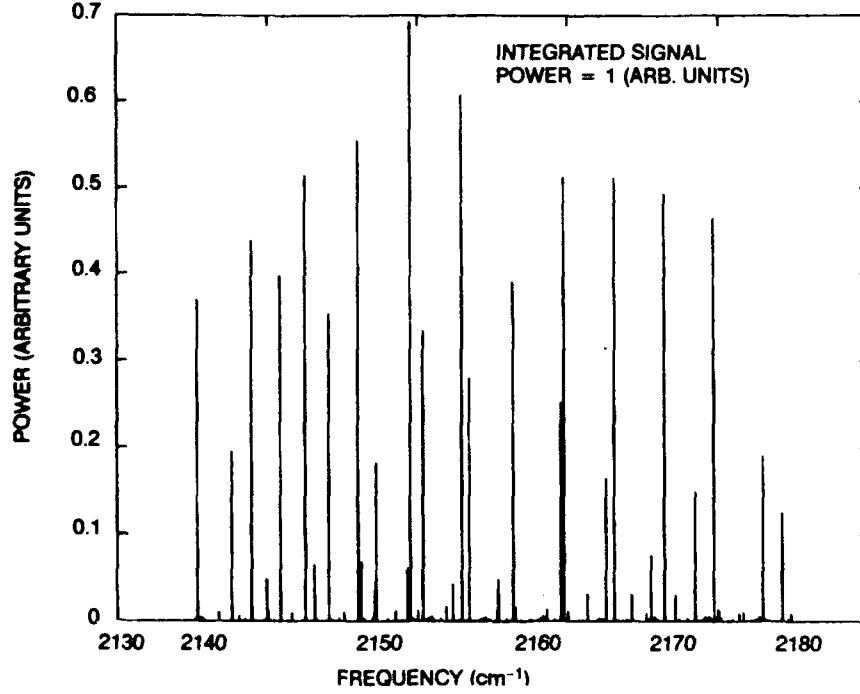


Figure 4. Signal Emission Spectrum

The transmission of the FP filter for radiation of frequency  $\nu$  and given mirror separation,  $\ell$ , is given by the well known Airy function, Equation (1)

$$T(\ell, \nu) = \frac{1}{1 + \frac{4}{\pi^2} \times \text{finesse} \times \sin^2 \delta / 2} \quad (1)$$

where  $\delta = 2\pi \ell \nu$ . The finesse is related to the mirror reflectance,  $R$ , by finesse =  $\pi \sqrt{R} / (1-R)$ . The total power transmitted by the FP,  $P_{\text{out}}(\ell)$ , is the convolution of the transmission (Airy) function and the power spectrum of the source,  $P_{\text{in}}(\nu)$ .

$$P_{\text{out}}(\ell) = \int_{\nu_1}^{\nu_2} T(\ell, \nu) P_{\text{in}}(\nu) d\nu \quad (2)$$

We have calculated the FP transmitted powers for both the signal and background spectra (Figs. 3 and 4) in the region of  $\ell$ , the mirror spacing, corresponding to maximum transmission of the signal spectrum. These are shown in Figs. 5a and 5b where the mirror separation (abscissa) was scanned 11  $\mu\text{m}$  to demonstrate several features of the FP comb filter.

In the signal spectrum (Fig. 5a), there are five nearly identical maxima. These correspond to maximum overlap of the FP with the CO emission spectrum. When the distance between the mirrors is increased or decreased much more, a mismatch occurs between the FP transmission peak spacing and the CO emission lines spacing, and the transmitted power decreases.

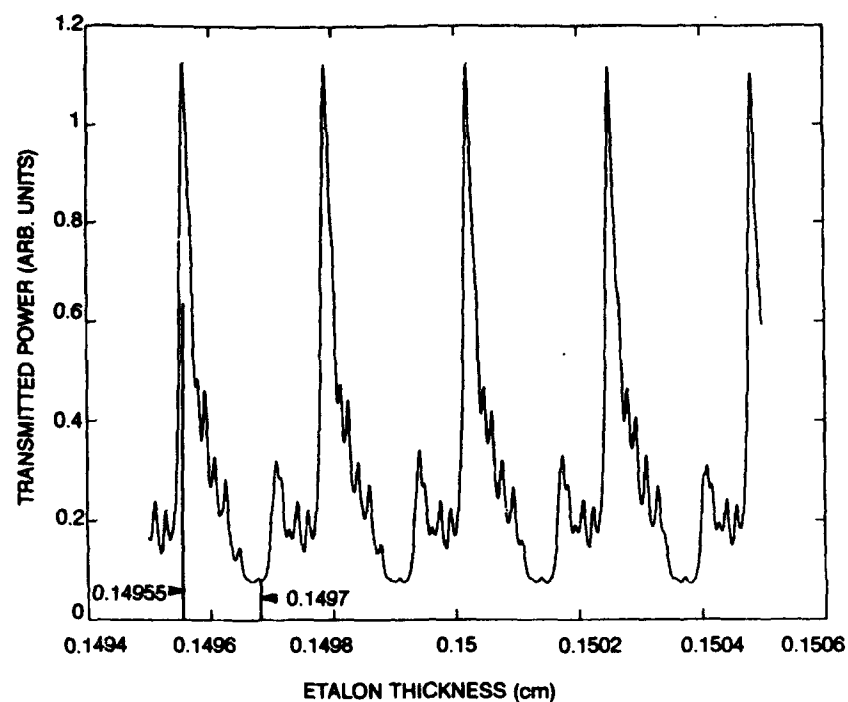


Figure 5a. Fabry-Perot Modulated Signal Spectrum, finesse = 25.  
( $P_{out}(\ell)$  from Eq. (2))

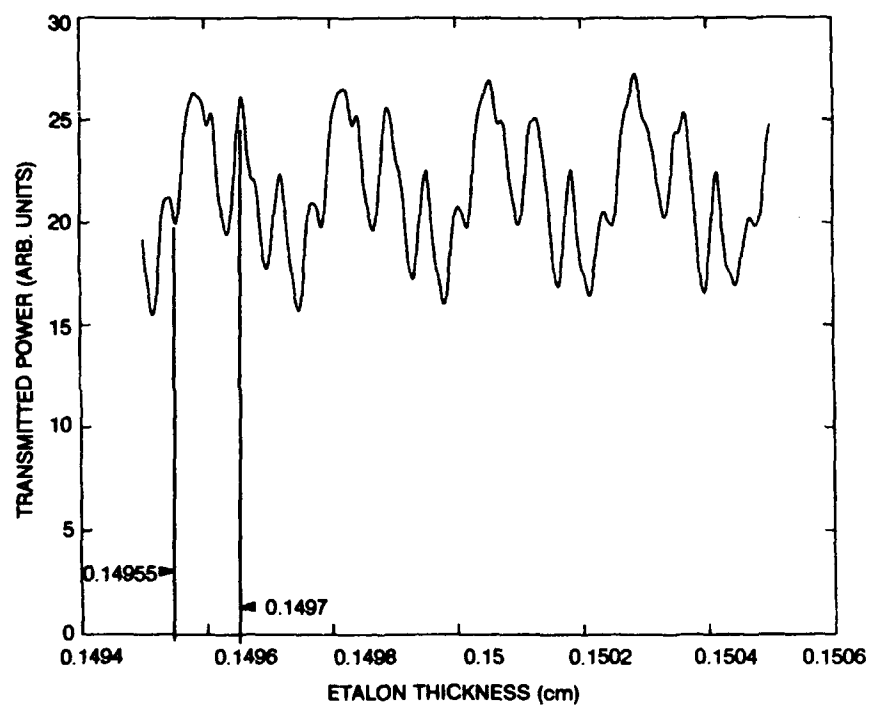


Figure 5b. Fabry-Perot Modulated Background Spectrum, finesse = 25.  
( $P_{out}(\ell)$  from Eq. 2)

The fraction of the signal and background powers transmitted by the FP (tuned to the first maximum) are tabulated in Table 1. Data for finesses of 0 (no FP filter) 25, 50, and 100 are given. (The convoluted spectra for finesse = 50 and 75 are shown in the Appendix.) With a finesse of 25, 26% of the signal power and 4.8% of the background power are transmitted, for a net improvement of 5.4 in the signal-to-background ratio. As shown in Table 1, improvements of 9.6 and 13.5 result from finesses of 50 and 100, respectively.

Table 1. Signal and Background With and Without Fabry-Perot Filter

Finesse	FP Signal Transmission (%)	Background Transmission (%)	Signal/Background (%)	Signal/Background Improvement
0 (no FP)	100%	100%	1.3%	1.0
25	26%	4.8%	7.0%	5.4
50	19%	1.9%	12.5%	9.6
100	13%	0.95%	17.5%	13.5

(spectrum = 2135 to 2175  $\text{cm}^{-1}$ )

The comb structure of the FP filter is not a perfect match to the slightly anharmonic CO emission lines. This is shown in the percent of the signal transmitted by the FP filter (the first column in Table 1). The transmitted signal level drops from 25% to 13% as the FP filter finesse increases from 25 to 100. However, in situations where background fluctuations are the dominant noise source, it is the signal/background ratio (the last column in Table 1) that determines the signal/noise ratio (see Section IV).

#### IV. SPECTRAL DITHERING

The spectral dithering invention requires the mirror separation to step back and forth between two positions. The first, position 1, corresponds to one of the maxima in the FP signal spectrum of Fig. 5a. The second, position 2, can be anywhere in the much broader minima of Fig 5a. The step size is very small, approximately 2  $\mu\text{m}$ .

We will estimate both the signal-to-background ratio and the signal-to-noise ratio improvement due to the FP for the case of a weak signal source,  $P_S$ , in the presence of a much larger background source,  $P_B$ , which fluctuates. The power transmitted by the FP at either position 1 or position 2 is the sum of two convolution integrals, which represent the transmitted power from the signal and background sources.

$$P_{\text{out}}(1) = T_1 * P_S + T_1 * P_B \quad (3)$$

$$P_{\text{out}}(2) = T_2 * P_S + T_2 * P_B \quad (4)$$

We have abbreviated the convolution integrals in Eq. (2) as \* products, and  $T_1$  is the FP transmission (Airy function) at position 1. ( $T_2$  is the transmission of the FP at position 2.)

The modulation imposed on the optical beam by spectral dithering is just the difference between  $P_{\text{out}}(1)$  and  $P_{\text{out}}(2)$

$$\Delta P = P_{\text{out}}(1) - P_{\text{out}}(2) \quad (5)$$

$$\Delta P = [T_1 * P_S - T_2 * P_S] + [T_1 * P_B - T_2 * P_B] \quad (6)$$

Equation (6) looks complicated, but it contains the essence of the spectral dithering invention. Each of the four terms is really just a point taken off of the plots in either Fig. 5a (for source,  $P_S$ , terms) or Fig. 5b (for background,  $P_B$ , terms).

Taking first the signal term ( $T_1 * P_S$ ), we want to pick position 1 at the peak of the CO emission signal. From Fig. 5a, we will take the first peak at a mirror spacing of 0.14955 cm (indicated in Fig. 5a), which corresponds to a transmitted power of 1.1 power units (proportional to watts). Temporarily, we will pick position 2 in the fairly broad minimum following the signal peak; at  $\ell = 0.1497$  cm and 0.07 power units. The mirror jump from position 1 to position 2 is  $1.5 \times 10^{-4}$  cm or 1.5  $\mu\text{m}$ . We can now calculate the first term in Eq. (6), the difference in signal power between positions 1 and 2, to be 1.03 power units.

In the same way, we can calculate the power due to the modulated background (the last two terms in Eq. (6)) using Fig. 5b (background) and the same mirror positions. The difference in background power at the two positions is  $21-23 = -2$  power units. Therefore, we have a signal-to-background ratio of approximately 1/2. This is a big improvement over the the 1/14 from the FP without spectral dithering. It appears that spectral dithering has improved the signal-to-background ratio by a factor of about 7 over the nondithered FP. However, we will show that this calculated improvement is somewhat arbitrary and depends primarily on the background fluctuations.

Position 2 can be picked anywhere in the signal minimum of Fig. 5a. By picking some other position within the *minimum*, it is possible to bring the background power at positions 1 and 2 arbitrarily close together. In the limit that they are equal, the signal-to-background ratio goes to infinity! This corresponds to perfect background subtraction. However, in the real world, the background changes while the FP is jumping from position 1 to position 2. The fluctuations due to atmospheric modulation are a function of the seeing conditions (time of day, elevation angle, aperture size, field-of-view and wavelength). Figure 6 shows the atmospheric modulation frequency spectrum obtained from stellar scintillations. Although this data was obtained at visible wavelengths, the course  $1/f$  dependence should be approximately correct for the CO emission. The percent modulation (the ordinate) will also depend on the seeing conditions.

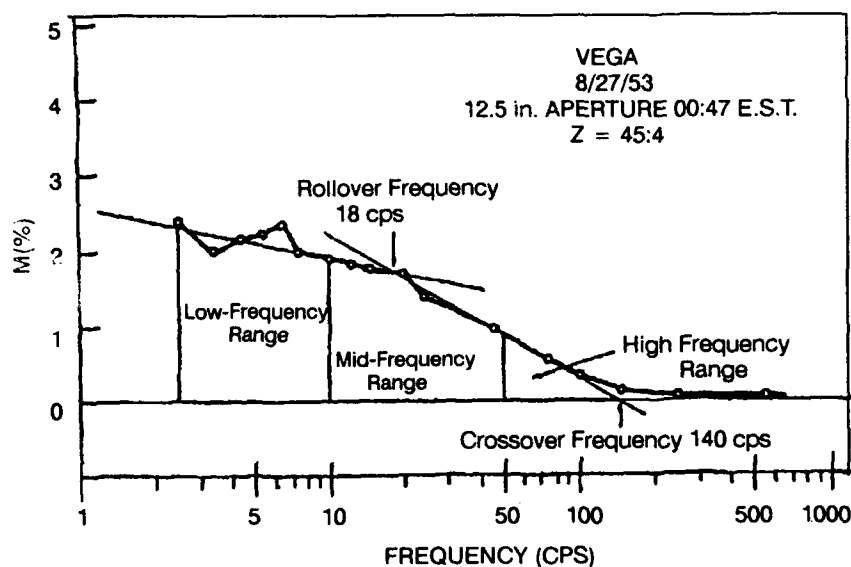


Figure 6. Atmospheric Modulation Spectrum.

We are interested in the case where the dominant noise source is the fluctuation in the background power due to atmospheric turbulence. The fluctuations are described by the fractional fluctuation,  $F_B(f)$ , where  $f$  is the fluctuation frequency.

The noise power,  $N$ , at either of the two mirror positions is just the transmitted background power at the two positions times the fractional fluctuation factor,  $F_B(f)$ .

$$N(1) = F_B(f)(T_1 * P_B) \quad (7)$$

$$N(2) = F_B(f)(T_2 * P_B) \quad (8)$$

As described above, by adjusting position 2,  $N(1)$  can be made approximately equal to  $N(2)$ . Therefore, the noise is the same at both mirror position and equal to Eq. (7) (or Eq. (8)).

$$N = F_B(P)(T_1 * P_B) \quad (9)$$



From Eq. (6), the modulated signal power is the difference in the transmitted signal powers at positions 1 and 2. We picked position 2 so that the transmitted signal power was very small; in our example, approximately zero. Therefore, the signal power  $S$  can be approximated as the transmitted signal power at position 1, which is just the first term in Eq. (6).

$$S = T_1 * P_S \quad (10)$$

The signal-to-noise ratio,  $S/N$ , is just the ratio of Eq. (10) to Eq. (9).

$$S/N \text{ (FP)} = \frac{T_1 * P_S}{F_B(f)(T_1 * P_B)} \quad (11)$$

For comparison purposes we need the  $S/N$  for the bandpass filter system.  $P_S$  and  $P_B$  are the signal and background powers transmitted through the filter.

$$S/N \text{ (BP)} = \frac{P_S}{F_B(f)(P_B)} \quad (12)$$

The FP filter with spectral dithering improves the  $S/N$  because the background subtraction occurs at 1 KHz as opposed to 10 Hz for typical telescope spatial dithering. We can use Fig. 6 to estimate the magnitude of this improvement. The fractional fluctuation decreases from about 2% to about 0.1% in going from 10 Hz to 500 Hz—a factor of 20! Even greater improvements could be expected when seeing conditions are poor (during mid-day, for instance).

At this point we have shown that the FP filter improves the signal-to-noise ratio by both reducing the transmitted background as shown in Table 1 (the comb filter effect) and by background subtracting at high frequencies ("freezing" the background fluctuations). The overall signal-to-noise ratio improvement is the product of these two effects. From Table 1, we see an improvement of 9.6 for a finesse of 50 and from Fig. 6, we estimated a factor of 20. The net improvement is 190!

## V. DEVELOPMENT OF AN FP FILTER FOR CO (CARBON MONOXIDE)

The ability of an FP to perform as described, depends primarily on two instrument capabilities: the reflective coatings on the mirrors, and the positioning accuracy of the mirror piezoelectric scanning drives.

We have purchased and tested a set of mirrors with a finesse of 30 for the  $3.7\text{--}5.7\text{ }\mu\text{m}$  region ( $1750\text{--}2700\text{ cm}^{-1}$ ). We have measured their finesse with a CO laser at  $5.42\text{ }\mu\text{m}$ . The finesse of 31.3 is readily measured as the ratio of the free spectral range (FSR) to the transmission peak width (FWHM), as shown with the oscilloscope traces in Fig. 7. Higher finessees are obtained by increasing the reflectance of the multilayer dielectric coatings. A finesse of 100 requires a mirror reflectance of 97%. We have assembled and tested a system with a finesse of 96 at  $10\text{ }\mu\text{m}$  as part of another program.

The mirrors were mounted in a Burleigh RC-150 Fabry-Perot system. The absolute distance between the mirrors was adjustable to within a few microns with three micrometer drives. Final positioning and the position jumping for spectral dithering were done with three piezoelectric drives that could scan up to 6 microns.

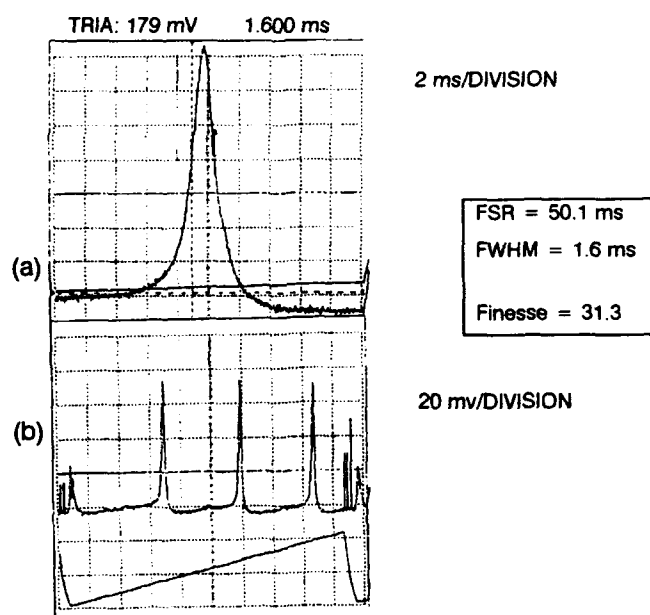


Figure 7. Measurement of FP Finesse of 31.3 with CO Laser at  $5.32\text{ }\mu\text{m}$   
(a) Full width at half-height measurement (b) FSR measurement.

## VI. SPECTRAL DITHERING DEMONSTRATION

An experiment to demonstrate spectral dithering was set up using the FP filter described in the previous section. A small propane-fueled torch was used as a hot CO source. The infrared emission from the flame was imaged on a 1 mm diameter InSb detector with an  $f/1$  ZnSe lens. The detector was fitted with a 4.5 to 5.0 micron bandpass filter, which transmitted the CO emission. The FP filter was placed immediately in front of the ZnSe lens. The FP filter was driven by a 600 Hz sine-wave oscillator.

The left-hand panel of Fig. 8 shows the output from the InSb infrared detector viewing the flame through the dithering FP filter. The large signal fluctuations are due to random fluctuations (flickering) of the flame. The timescale for fluctuation noise is approximately 0.05 sec, or 20 Hz. It would be difficult to estimate the amount of CO emission from this signal both because it fluctuates and because it may contain some blackbody emission from soot particles in the flame.

The right-hand panel of Fig. 8 shows a small portion of the signal in the left-hand panel on an expanded scale. At the bottom of the right-hand panel is the modulation signal that drives the piezo elements in the dithering FP filter. Above it, one can see that the expanded view of the infrared signal is indeed modulated in phase with the FP drive. This signal is due to CO emission. It is strongly affected by the air/gas mixture in the flame, and is significantly reduced by the insertion of a CO cold gas filter in front of the FP filter. The sine-wave-modulated signal in the right-hand panel of Fig. 8 is a fingerprint for CO emission.

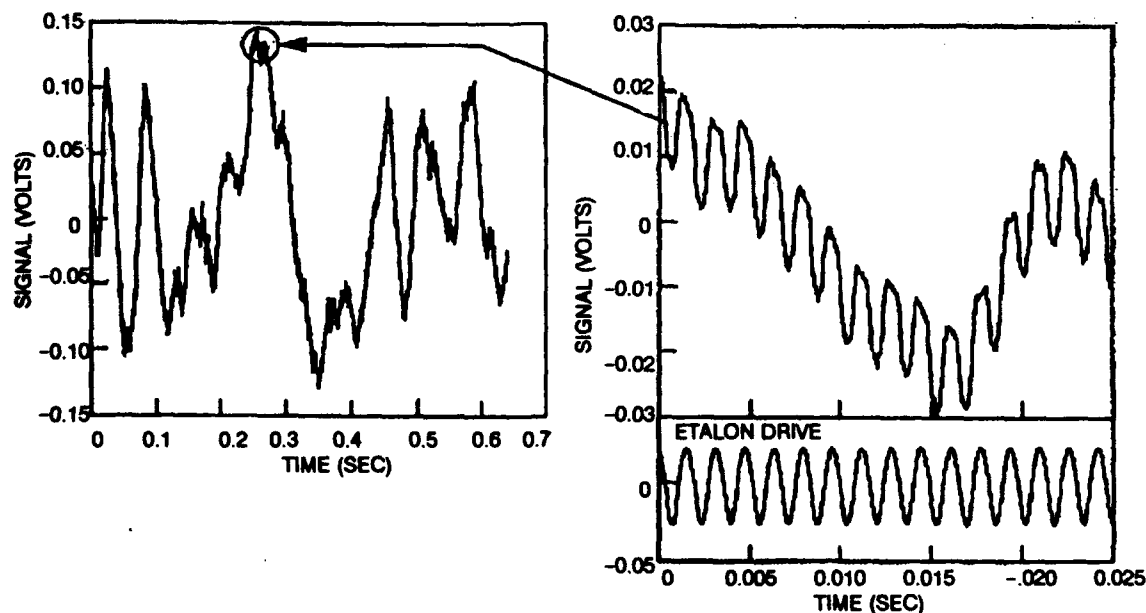


Figure 8. FP Modulated Emission Spectrum for a Small Gas Flame. In the left panel, the IR emission fluctuates due to turbulence. The right panel shows the modulated signal due to the spectral dithering FP filter.

## VII. SUMMARY

The FP filter is a comb filter that can be matched to the regularly spaced infrared-molecular emission lines. This significantly improves the signal-to-noise ratio by two mechanisms. First, the comb nature of the filter rejects the background radiation that falls between the regularly spaced lines. For CO emission the comb filter effect improves the signal-to-background ratio by more than a factor of 10 (see Table 1). Second, the spectral dithering invention is a fast ( $\sim 1$  millisecond) background subtraction technique that essentially freezes the background. When background fluctuations are a significant noise source, signal-to-background ratio improvements will translate into signal-to-noise ratio improvements. Large signal/noise improvements are expected because the effects of the two mechanisms are multiplicative. In addition, the FP filter offers a significant "recognition advantage" because the modulated signal pattern is unique to a specific molecule. Finally, the FP filter can operate in either a single pixel or an imaging optical system.

## REFERENCES

1. J. T. Houghton, "The Meteorological Significance of Remote Measurements of the Infrared Emission From Atmospheric Carbon Dioxide," *Quant. J. Roy. Met. Soc.* **87**, p. 102-104 (1960).
2. S. D. Smith, "Design of Interference Filters for the Observation of Infrared Emission from Atmospheric Carbon Dioxide by an Earth Satellite," *Quant. J. Roy. Met. Soc.* **87**, p. 431-434 (1961).
3. C. M. Randall, P. F. Zittel, L. A. Darnton, and F. S. Simmons, "Evaluation of the Fabry-Perot Etalon for Spectral Discrimination in IR Surveillance," *SPIE* **253**, p. 212-220 (1980).
4. C. M. Randall, P. F. Zittel, and L. A. Darnton, "Evaluation of the Fabry-Perot Etalon for Spectral Discrimination in Infrared Surveillance Systems," Final Report ATR-79(8328-02)-1, The Aerospace Corporation (1979).

## APPENDIX

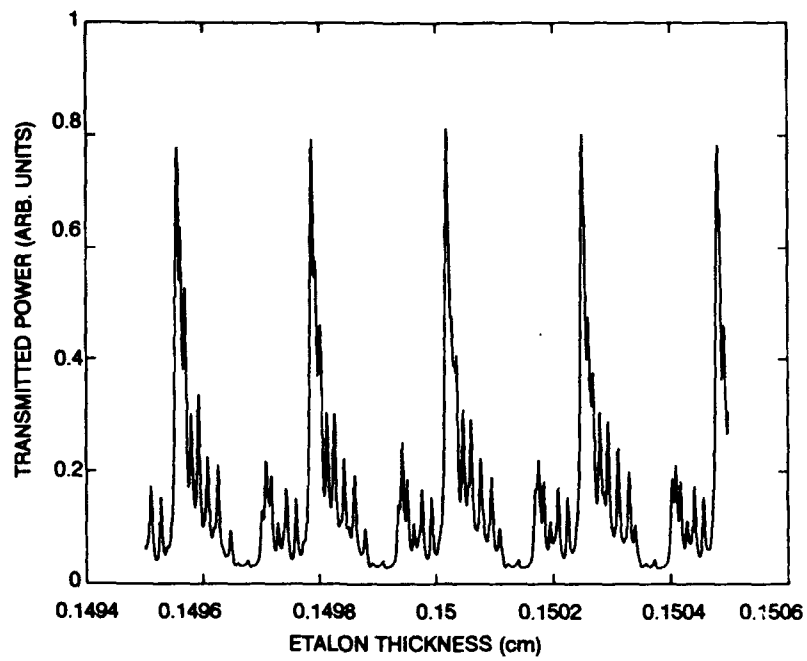


Figure A1a. Fabry-Perot Modulated Signal Spectrum (finesse = 50)

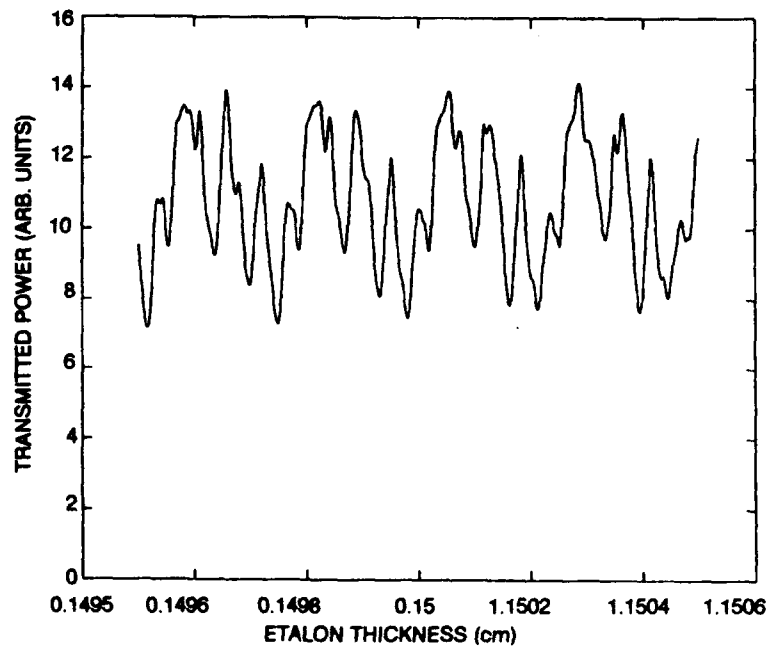


Figure A1b. Fabry-Perot Modulated Background Spectrum (finesse = 100)

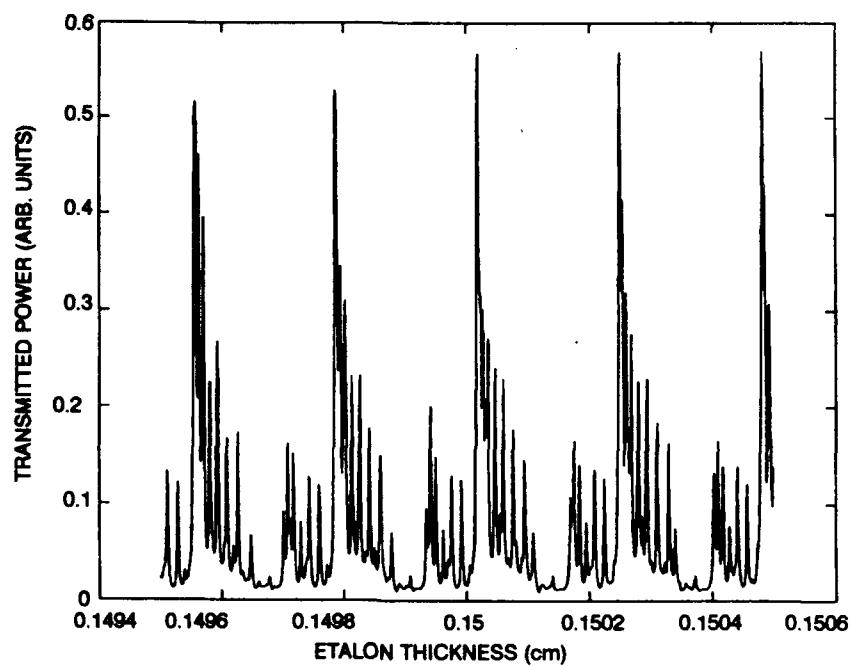


Figure A2a. Fabry-Perot Modulated Signal Spectrum (finesse = 100)

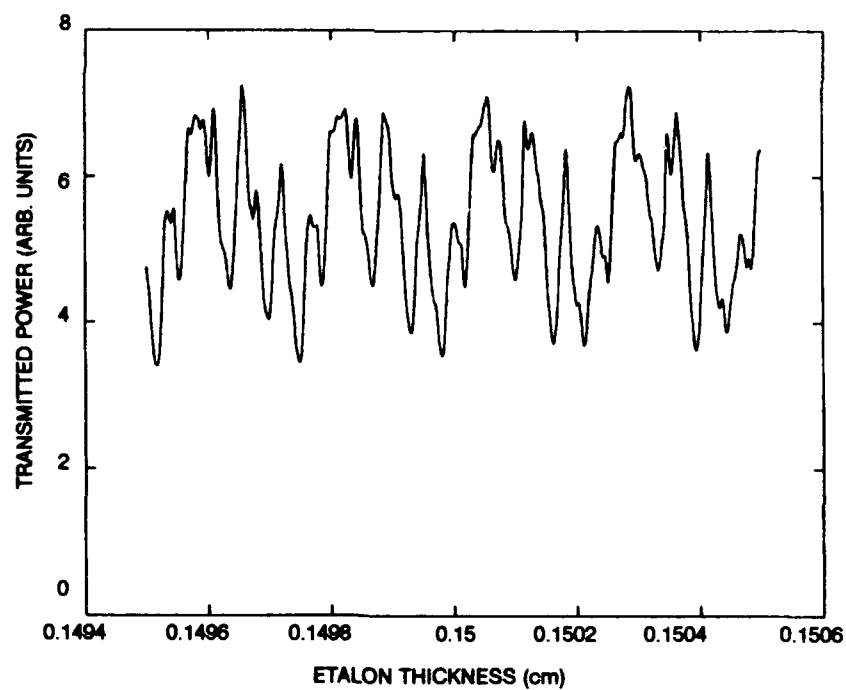


Figure A2b. Fabry-Perot Modulated Background Spectrum (finesse = 100)

## **TECHNOLOGY OPERATIONS**

The Aerospace Corporation functions as an "architect-engineer" for national security programs, specializing in advanced military space systems. The Corporation's Technology Operations supports the effective and timely development and operation of national security systems through scientific research and the application of advanced technology. Vital to the success of the Corporation is the technical staff's wide-ranging expertise and its ability to stay abreast of new technological developments and program support issues associated with rapidly evolving space systems. Contributing capabilities are provided by these individual Technology Centers:

**Electronics Technology Center:** Microelectronics, solid-state device physics, VLSI reliability, compound semiconductors, radiation hardening, data storage technologies, infrared detector devices and testing; electro-optics, quantum electronics, solid-state lasers, optical propagation and communications; cw and pulsed chemical laser development, optical resonators, beam control, atmospheric propagation, and laser effects and countermeasures; atomic frequency standards, applied laser spectroscopy, laser chemistry, laser optoelectronics, phase conjugation and coherent imaging, solar cell physics, battery electrochemistry, battery testing and evaluation.

**Mechanics and Materials Technology Center:** Evaluation and characterization of new materials: metals, alloys, ceramics, polymers and their composites, and new forms of carbon; development and analysis of thin films and deposition techniques; nondestructive evaluation, component failure analysis and reliability; fracture mechanics and stress corrosion; development and evaluation of hardened components; analysis and evaluation of materials at cryogenic and elevated temperatures; launch vehicle and reentry fluid mechanics, heat transfer and flight dynamics; chemical and electric propulsion; spacecraft structural mechanics, spacecraft survivability and vulnerability assessment; contamination, thermal and structural control; high temperature thermomechanics, gas kinetics and radiation; lubrication and surface phenomena.

**Space and Environment Technology Center:** Magnetospheric, auroral and cosmic ray physics, wave-particle interactions, magnetospheric plasma waves; atmospheric and ionospheric physics, density and composition of the upper atmosphere, remote sensing using atmospheric radiation; solar physics, infrared astronomy, infrared signature analysis; effects of solar activity, magnetic storms and nuclear explosions on the earth's atmosphere, ionosphere and magnetosphere; effects of electromagnetic and particulate radiations on space systems; space instrumentation; propellant chemistry, chemical dynamics, environmental chemistry, trace detection; atmospheric chemical reactions, atmospheric optics, light scattering, state-specific chemical reactions and radiative signatures of missile plumes, and sensor out-of-field-of-view rejection.